Influence of Acceptor Side-Chain Length and Conjugation-Break Spacer Content on the Mechanical and Electronic Properties of Semi-Random Polymers

Elizabeth L. Melenbrink,[a] Kristan M. Hilby,[b] Kartik Choudhary,[b] Sanket Samal,[a] Negar Kazerouni,[a] John Luke McConn,[a] Darren J. Lipomi,[b] and Barry C. Thompson[a]**

[a]Department of Chemistry and Loker Hydrocarbon Research Institute, University of Southern California, Los Angeles, California 90089-1661

[b]Department of NanoEngineering, University of California San Diego, 9500 Gilman Drive, Mail Code 0448, La Jolla, CA 92093-0448, United States

*Email: barrycth@usc.edu

*Email: dlipomi@eng.ucsd.edu

Keywords: Conjugated polymers, conjugation-break spacer, semi-random polymers, mechanical properties, film-on-water

Abstract:

Conjugation-break spacers (CBS) have been shown to enhance the mechanical properties of conjugated polymers. In particular, incorporation of CBS units into semi-random polymers has revealed high ductility and low elastic moduli, attributed to the combined influence of the CBS units and the semi-random architecture. To further elucidate the structure-property relationships in these polymers, two new families of semi-random polymers are reported here. In the first, poly(3-hexylthiophene)-based semi-random polymers incorporating diketopyrrolopyrrole (DPP) units were synthesized in which CBS units with 4-10 carbons were incorporated from 10-40% with an equivalent content of 2-decyltetradecyl-DPP (dtdDPP) in order to overcome solubility limitations previously observed with 2-ethylhexyl-DPP (ehDPP). These polymers had much higher solubility and could attain higher molecular weights, formed films with high integrity, and displayed extraordinary mechanical properties, with elastic moduli as low as 5.45 MPa and fracture strains as high as 398%. In the second family, the content of ehDPP was held constant at 10%, while the CBS content was varied from 10-50% (with an 8-carbon spacer) in order to deconvolute the influence of CBS and DPP content on mechanical properties. Polymer solubility, molecular weight, and processability were not shown to improve dramatically relative to the previous generation of ehDPP polymers with matched DPP and CBS content, but the mechanical properties of this series were quite notable, with elastic moduli as low as 4.08 MPa, an increase in toughness, and fracture strains as high as 432%. The extraordinary mechanical properties exhibited by these polymers can serve as a guide in the judicious selection of monomers and backbone architectures in the future synthesis of semiconducting polymers for flexible electronic applications.

Introduction:

Recently, conjugation-break spacers (CBS) have been incorporated into conjugated polymers to impart such advantages as solubility,[1,2] melt processability,[3,4] and molecular weight-independent optoelectronic properties.[5-7] Several studies, including our own, have shown that CBS units greatly impact mechanical properties relative to fully conjugated polymers without significant detriment to the favorable electronic characteristics that make conjugated polymers attractive as semiconductors.[8-10] Prior studies have connected factors such as solid state packing arrangement and molecular structure to mechanical properties, including elastic modulus (E).[8] Materials with lower elastic moduli are expected to deform more easily and produce less interfacial stress in a multi-layered device, reducing the likelihood of device failure by interfacial delamination. For this reason, these materials are generally regarded as better for use in flexible electronic applications.[10] Although fully conjugated polymers demonstrate a wide range of elastic moduli (E = 0.1−8 GPa),[9,11-14] polymers incorporating CBS units have generally exhibited values lower than 1 GPa.[8-10] Though these values are low for semiconducting polymers, they are still orders of magnitude higher than that of typical elastomers such as polydimethylsiloxane (0.6-2.5 MPa)[15] and polyisoprene (0.36 MPa).[16]

To date, most CBS studies, particularly those in which mechanical properties are measured, have used AA/BB functionalized monomers to make perfectly alternating or semi-alternating[17] (random) conjugated polymers.[7-9] In contrast, our studies use semi-random polymers with AA, AB, and BB functionalized monomers. This allows monomers more freedom in the manner in which they can bond to each other, which increases disorder along the polymer backbone, manifesting in bulk properties such as crystallinity.[18] This increased disorder is expected to enhance the mechanical properties of thin films of conjugated polymers that are known for being

stiff and brittle.[11-13,19,20] Our previous work showed that combining conjugation-break spacers and a semi-random polymer architecture resulted in elastic moduli as low as 0.13 GPa and crack-onset strains (COS) as high as 80%.[10] In addition to the mechanical advantages conferred by the semi-random architecture, the less restrictive linkage pattern has also been shown to broaden optical absorption relative to precisely alternating conjugated polymers by engendering a larger distribution of chromophores in of the polymer.[21] Finally, by utilizing 3-hexylthiophene as the AB functionalized monomer, the beneficial characteristics of P3HT, including absorption, surface energy, and frontier orbital energies can be retained.[18,21,22]

In our previous study, semi-random CBS polymers were synthesized with a structure based on a highly successful polymer previously studied in our group, P3HTT-DPP-10% (**Scheme 1**). The distannylthiophene monomer was replaced with a distannyl T-X-T monomer, where X indicates a hydrocarbon spacer length of 4, 6, 8, or 10 methylene units between two thiophenes. The content of the CBS monomer was varied concurrently with the DPP monomer (with 2-ethylhexyl side chains) at 10%, 20%, 30%, and 40%, with a corresponding 3-hexylthiophene content of 80%, 60%, 40%, and 20%. The 10% T-10-T polymer provided an especially promising result with an elastic modulus of 0.13 GPa (film-on-water), a COS of > 80% (film-on-elastomer), and a hole mobility of 2.53 x 10^{-4} cm^2 V^{-1} s^{-1}, which was comparable to the fully conjugated analogue (9.29 x 10^{-4} cm^2 V^{-1} s^{-1}). Despite these encouraging mechanical and electronic results, our previous semi-random CBS polymers were hampered by poor solubility (especially for those with higher DPP and CBS content), which limited molecular weight and film-forming capacity. This in turn affected our ability to complete measurements of charge mobility and mechanical properties for all samples. We noted that the solubility of our polymers decreased with increasing fraction of CBS monomer

in the backbone, contrary to the findings of Zhao et. al,[3] which we attributed to the concurrent increase in DPP incorporation in the backbone.

Scheme 1. Previously studied semi-random polymers.

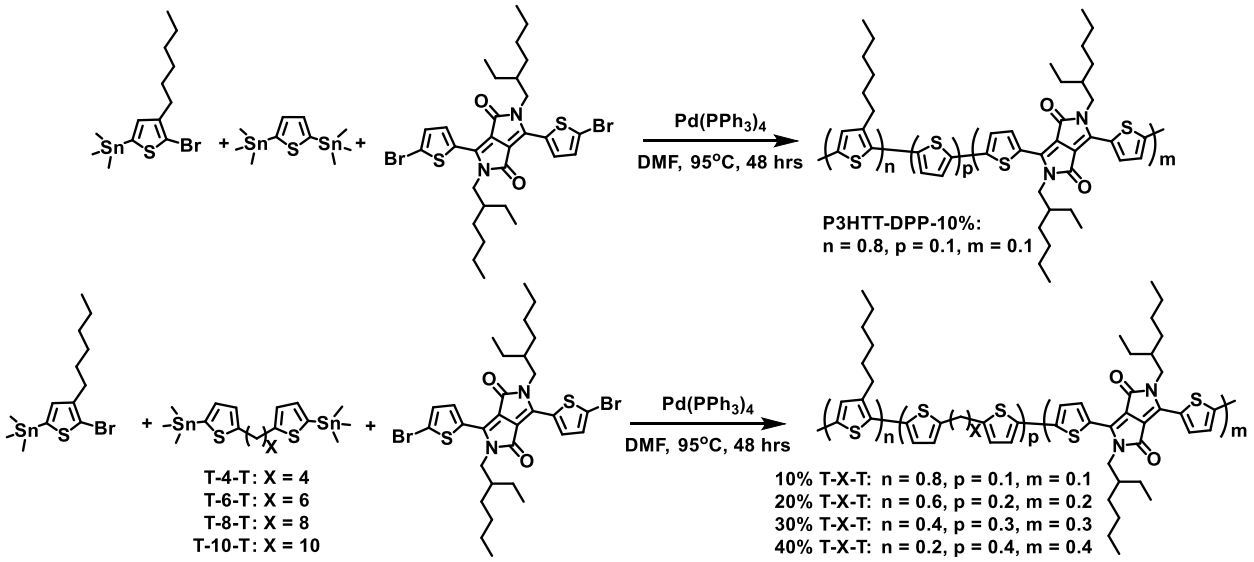

In order to address the solubility and further elucidate the structure-property relationships of semi-random CBS polymers, here we synthesized two families of polymers. In the first (**Scheme 2a**) we have prepared the direct analogues of select members of the previously reported family (**Scheme 1**) in which we have replaced the 2-ethylhexyl (eh) side chains of DPP with 2-decyltetradecyl (dtd). We hypothesized that the longer side-chains on DPP would allow for higher molecular weight polymers to be synthesized due to increased solubility, and we anticipated that the polymers with higher CBS and DPP contents would thus be better able to form films for mechanical and mobility studies. Additionally, alkyl side-chains (nominally used to confer solubility) have been shown to have a strong influence on mechanical properties with branched and flexible side-chains yielding the most favorable metrics with respect to deformability.[11,23] As

a result, an increase in stretchability was expected as the length of the side-chain increased. However, longer side-chains were also expected to have detrimental effects on optoelectronic properties as a result of increased weight fraction of insulating hydrocarbons and increased distance between polymer backbones. This phenomenon has been well-established in the literature, with longer and bulkier side-chains generally leading to a decrease in charge mobility and absorption coefficient for conjugated polymers.[24,25] However, a few examples exist in which longer side-chains contributed to an improvement in molecular packing, which in turn enhanced the charge mobility and other optoelectronic properties.[26-28]

Scheme 2. Semi-random polymers synthesized for this study. a) Eight CBS polymers and one fully conjugated reference polymer with decyltetradecyl DPP side-chains; b) Five CBS polymers with fixed ethylhexyl DPP content and variable T-8-T content.

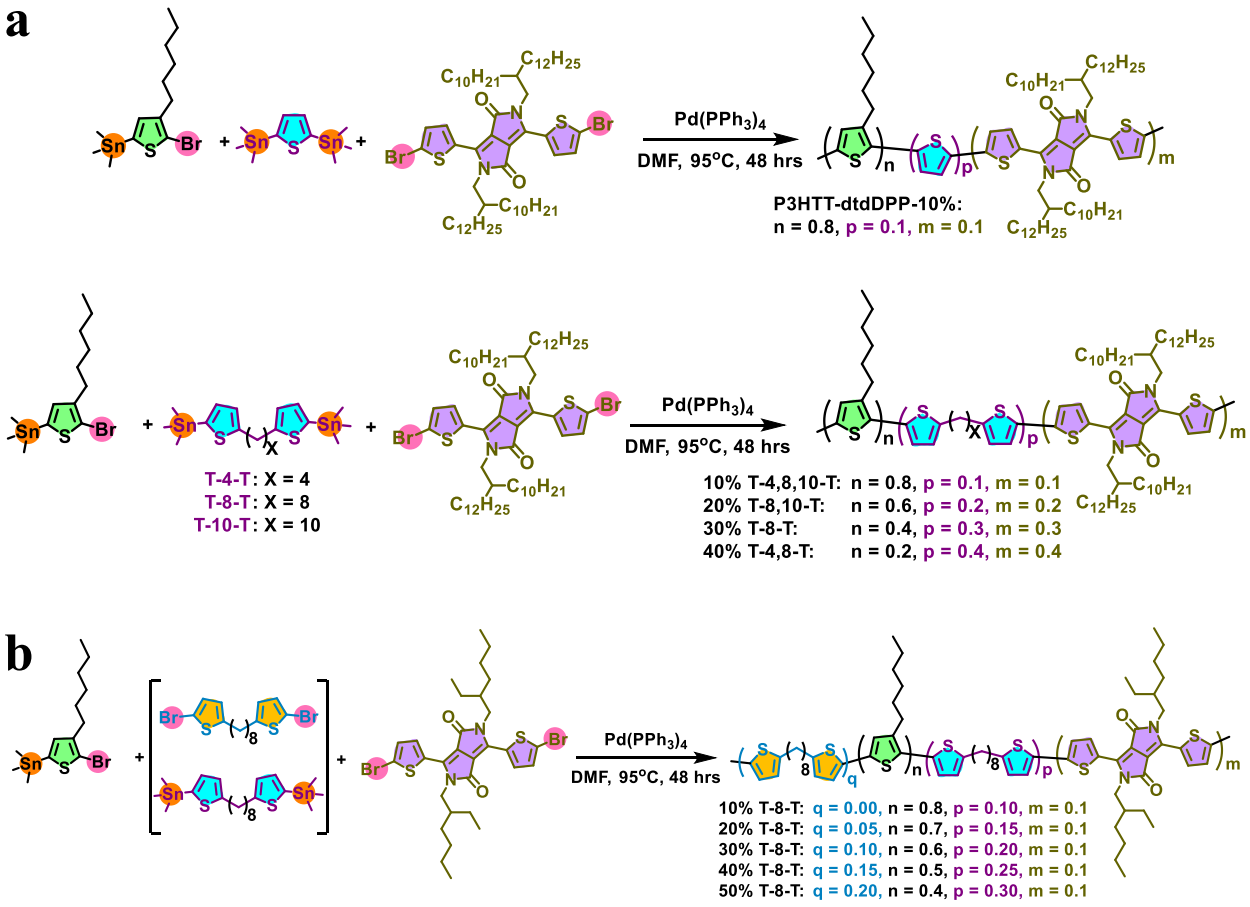

In our past work on semi-random polymers we have shown that increasing the content of ehDPP units results in decreasing solubility.[22] In order to target improved solubility at high CBS contents and to deconvolute the influence of CBS and DPP content, we sought to study the effect of increasing CBS content without the simultaneous increase in DPP content and without the need for using longer side chains. As such, we developed the family of polymers in **Scheme 2b**. In the previous family (**Scheme 1**), due to the AA/AB/BB functionality of the three monomers used, the DPP acceptor content was tied to the CBS content to maintain stoichiometric balance. However, it appeared that increasing the DPP and CBS monomers simultaneously had competing effects on solubility, electronic properties, and mechanical properties, where solubility was found to decrease as DPP and CBS content increased.[10] Therefore, a second conjugation-break spacer monomer with dibromo functionality was added so that DPP content could remain constant while increasing CBS content (**Scheme 2b**). The DPP monomer content was fixed at 10 mole percent to minimize negative effects from DPP on solubility and mechanical properties, and because the 10% DPP polymers from our previous study had the highest charge carrier mobiltiy.[10] We anticipated that this polymer family would have improved solubility and mechanical properties when compared to the T-8-T family of polymers that was synthesized with variable ehDPP content. Both families of polymers exhibited a marked improvement in mechanical properties relative to our first CBS study, allowing us to deduce that judicious selection of monomers and backbone architectures may result in better semiconducting polymers for flexible electronic applications.

Results and discussion:

Effects of side-chain length: decyltetradecyl DPP vs ethylhexyl DPP

A series of eight polymers with different compositions of the CBS, dtdDPP, and 3-hexylthiophene monomers was synthesized via Stille polymerization,[21] along with the reference polymer, P3HTT-dtdDPP-10% **(Scheme 2a)**. As with our previous study,[10] alkyl chains with an even number of carbons were exclusively studied to eliminate the possibility of an odd-even effect[29] and for economic practicality. Polymers were named for the CBS monomer length and content as well as the corresponding dtdDPP content. For example, a polymer with a 4-carbon CBS incorporated into the backbone at 10 mole percent, 10 mole percent of dtdDPP, and 80 mole percent of 3HT would be named 10% T-4-T/10% dtdDPP. A smaller selection of polymers was targeted for this follow-up study than for the previous study including: (i) all of the T-8-T sub-family (10-40%) for comparison with the polymers in **Scheme 2b** as well; (ii) bookends (10% and 40%) of the T-4-T family because that family exhibited the worst solubility with ehDPP; and (iii) the lower CBS fractions (10-20%) of the T-10-T family due to their favorable electronic properties in our previous study. ^{1}H NMR was used to confirm that the monomer feed ratios matched the polymer composition (**Figure S7-S10**). Higher molecular weights were attained throughout the dtdDPP family (M_n = 20.9 – 47.6 kDa, **Table 1, Table S1, Figure S1**) when compared to the ehDPP family (M_n = 6.4 – 29.0 kDa),[10] and the fully conjugated polymer had the lowest molecular weight in this family (M_n = 14.9 kDa). The lower molecular weight of the P3HTT-dtdDPP-10% polymer is attributed to poor solubility and suggests that the CBS monomers indeed enhanced the solubility of this family, a trend which could not clearly be seen in our first study. Interestingly, as the fraction of the alkyl spacers and dtdDPP in the polymer increased, so too did the polymerization yields (**Table S2**), a trend also likely linked to solubility. For those polymers with low CBS and

dtdDPP content, large amounts of the polymers (with molecular weights as high as 7 kDa, much higher than the 2-3 kDa typically observed in fully conjugated polymers) were extracted into the hexane Soxhlet fractions giving hexane yields of 30-50%. These high hexane yields reduced the yield in the subsequent chloroform Soxhlet fraction. Lower hexane yields and higher chloroform yields were generally attained at higher CBS and dtdDPP incorporation (**Figure S2**), indicating that those polymers were less soluble in hexane, though they still dissolved readily in halogenated organic solvents.

Table 1. SEC, thermal, optical, and electronic data for decyltetradecyl DPP polymers

Polymer	**M_n[a]** (kDa)	**Đ[a]**	**T_m / T_c[b]** (°C)	**E_g[c]** (eV)	**HOMO[d]** (eV)	**$\mu_{h,\ annealed}$[e]** ($cm^2\ V^{-1}\ s^{-1}$)	**$\mu_{h,\ as\text{-}cast}$[f]** ($cm^2\ V^{-1}\ s^{-1}$)
P3HTT-dtdDPP-10%	14.9	3.24	150 / 143	1.51	5.62	6.11 E-4	4.24 E-4
10% T-4-T/10% dtdDPP	29.9	2.20	108 / 93	1.54	5.55	4.56 E-6	2.91 E-6
10% T-8-T/10% dtdDPP	26.1	3.90	- / -[g]	1.56	5.59	5.03 E-5	3.95 E-5
10% T-10-T/10% dtdDPP	33.0	3.27	- / -[g]	1.56	5.57	7.77 E-5	6.57 E-5
20% T-8-T/20% dtdDPP	35.5	2.59	72 / 50	1.62	5.56	2.14 E-5	1.01 E-5
20% T-10-T/20% dtdDPP	31.1	5.05	56 / 33	1.63	5.59	1.57 E-5	1.14 E-5
30% T-8-T/30% dtdDPP	47.6	2.37	103 / 64	1.67	5.52	-[h]	6.22 E-6
40% T-4-T/40% dtdDPP	20.9	2.86	164 / 140	1.68	5.57	-[h]	1.65 E-6
40% T-8-T/40% dtdDPP	44.1	2.54	120 / 86	1.71	5.54	-[h]	4.92 E-6

a) Obtained through size-exclusion chromatography (SEC); b) Obtained through differential scanning calorimetry (DSC); c) Calculated from the absorption onset in annealed thin films; d) Calculated from cyclic voltammetry (CV) oxidation onset; e) Calculated from charge carrier mobility measurements in the space charge limited current (SCLC) regime in hole-only devices in which the polymer thin film was spin-cast from chloroform and annealed for 30 min at 150 °C prior to cathode deposition; f) Calculated from charge carrier mobility measurements in the space charge limited current (SCLC) regime in hole-only devices in which the polymer thin film was spin-cast from chloroform and left under N_2 for 30 min prior to cathode deposition; g) No thermal transitions observed; h) Hole mobility could not be consistently measured.

The thin-film UV-vis spectra of the polymers in the T-8-T/dtdDPP family (**Figure 1a**) are representative of the trends observed in this study. UV-vis spectra for all the polymers, as-cast and annealed, are provided in **Figures S13-S20**. Similar to the previous study, all of the CBS polymers had a wider optical bandgap and blue-shifted absorption onset when compared to P3HTT-dtdDPP-10%, which contains no conjugation break spacers (**Table 1**). The absorption onset blue-shifted linearly as the content of dtdDPP and CBS increased, to the maximum bandgap of 1.71 eV for 40% T-8-T/40% dtdDPP (**Table S8, Figure S22**). As expected, the optical bandgaps are not dependent on the length of the DPP side-chain and the values presented herein are virtually the same as those reported for the polymers with ethylhexyl side-chains on the DPP monomer.[10] Similar to what we reported previously, the length of the spacer appeared to have no effect on the absorption onset. However, thermal annealing led to a slight increase in the bandgap for most of the samples, as evidenced by the blue-shift in absorption (**Tables S5-S6**). All absorption coefficients for the new family of polymers were lower than those obtained for the previous family of polymers (**Tables S5-S6**). This is as expected, for the longer side-chains on DPP make it so that there is less electroactive polymer per unit volume than for the polymers with shorter side-chains.

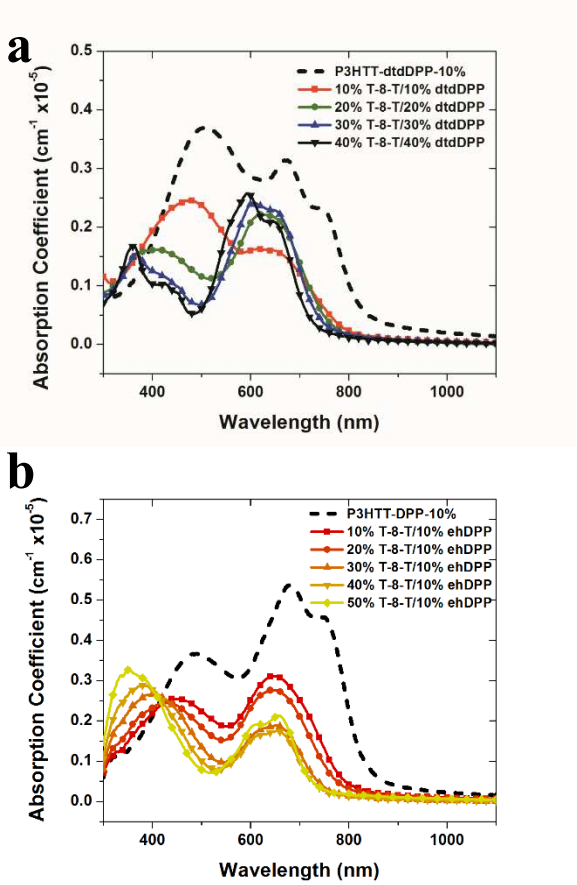

Figure 1. (a) UV-Vis absorption spectra for the T-8-T/dtdDPP series of polymer thin films spin-cast from chloroform and annealed under N_2 at 150 °C for 30 minutes. (--) P3HTT-dtdDPP-10% fully conjugated reference polymer; (■) 10% T-8-T/10% dtdDPP; (●) 20% T-8-T/20% dtdDPP; (▲) 30% T-8-T/30% dtdDPP; (▼) 40% T-8-T/40% dtdDPP. (b) UV-Vis absorption spectra for the T-8-T/10% ehDPP series of polymer thin films spin-cast from *o*-dichlorobenzene (*o*-DCB) and annealed under N_2 at 150 °C for 30 minutes. (--) P3HTT-DPP-10% fully conjugated reference polymer; (■) 10% T-8-T/10% ehDPP; (●) 20% T-8-T/10% ehDPP; (▲) 30% T-8-T/10% ehDPP; (▼) 40% T-8-T/10% ehDPP; (♦) 50% T-8-T/10% ehDPP.

The high melting and crystallization temperatures observed with the reference ehDPP-based P3HTT-DPP-10% (T_m = 208 °C; T_c = 182 °C)[10] were significantly depressed in the fully

conjugated P3HTT-dtdDPP-10% (T_m = 150 °C; T_c = 143 °C) when analyzed by differential scanning calorimetry (DSC) (**Table 1, Figure S34**). As in our previous study, thermal transitions were not observed for most of the 10% T-X-T polymers. Many of the dtdDPP polymers that exhibited thermal transitions in this study did not display such transitions in the polymers of the same composition with shorter side-chains.[10] This makes it difficult to draw comparisons between the two families. Within the T-8-T/dtdDPP sub-family, however, a clear trend appeared in which the melting and crystallization temperatures rose with increasing CBS and DPP incorporation (**Tables S15-S16, Figures S43-S44**). This mirrors the trend that was seen in the family of polymers with shorter side-chains. Because the equilibrium melting point of a polymer is inversely related to the entropy of fusion for melting,[30] the increasing melt and crystallization temperatures of this polymer family indicated that the entropy of these transitions was decreasing as DPP and CBS content increased. This decrease in entropy was perhaps due to a decrease in chain flexibility,[29] which is most reasonably attributed to the rise in DPP monomer content, as the conjugation-break spacer was expected to enhance polymer chain flexibility. This opposes the trend that emerged with increasing CBS length, in which the entropy of the thermal transitions increased, thus depressing melting and crystallization temperatures, as we observed in our previous study.[10]

Crystallinity was investigated in thin films of T-X-T/dtdDPP polymers via grazing incidence X-ray diffraction (GIXRD). While weak diffraction peaks were observed for the majority of the polymers in as-cast films (**Figure S51, Table S19**), after annealing (150 °C, 30 minutes) the weak peaks disappeared. Intense diffraction peaks were observed only for those polymers incorporating 40% CBS and dtdDPP (**Figure S52, Table S20**). The 100 diffraction peaks for as-cast films corresponded to a lamellar packing distance of 17.3-20.4 Å, larger than the range of 15.6-16.5 Å observed in our original study for ehDPP analogues. This can be explained by the longer DPP side-

chains generally causing the polymer chains to pack further apart, a phenomenon previously observed in our group when exchanging ethylhexyl side-chains for decyltetradecyl side-chains.[31] Within the T-8-T/dtdDPP subfamily, a trend appeared in the as-cast films in which the lamellar packing distance decreased with increasing CBS and dtdDPP incorporation. Although the fraction of monomer with long side-chains was increasing within this data set, it seemed that increasing the CBS content allowed the polymer chains to pack closer together, likely due to the enhanced open space provided by the increased fraction of CBS, and counter to the trend observed by Ekiz et al. when increasing DPP content without the use of a CBS monomer.[31] Interestingly, there is no observed diffraction peak for the fully conjugated polymer before annealing. These results pointed to the conjugation-break spacer as a key factor in polymer crystallinity, perhaps imbuing the conjugated segments of the backbone with enough flexibility to arrange themselves in a manner favorable for π-π stacking. It is curious that order seemed to disappear in most samples upon annealing, although the intensity of the 40% CBS/40% dtdDPP samples increased greatly, to the point that we could even observe a 200 reflection in the 40% T-4-T/40% dtdDPP annealed film. Upon annealing, the lamellar packing distance of 40% T-4-T/40% dtdDPP diminished slightly from 20.4 Å to 20.1 Å, whereas for 40% T-8-T/40% dtdDPP lamellar packing distance decreased from 17.3 Å to 15.9 Å, once again likely due to the enhanced open space between chains when longer spacers are present. Presumably the greater flexibility lent to the polymer by the longer (eight-carbon) CBS allowed the polymer backbones to draw closer to each other during annealing than was possible for the polymer with a shorter (four-carbon) CBS.

The HOMO of each polymer was estimated from the onset of oxidation using cyclic voltammetry (CV). No trends were observed in the HOMOs of these polymers, as demonstrated by the data presented in **Table 1** and **Figure S31**. When averaged across the entire range of CBS

polymers in this study, the HOMO was 5.56 ± 0.02 eV, which is well within the measurement error of ± 0.05 eV, and indicative of how closely clustered the data set was. This average CBS polymer HOMO was slightly shallower than the 5.62 eV HOMO of the fully conjugated reference polymer, P3HTT-dtdDPP-10%, mirroring the trend observed in the first study,[10] with the exception that all HOMO energies are approximately 0.1 eV deeper for the polymers with longer DPP side-chains. Although several studies have investigated the effects of side-chain length on electronic properties of conjugated polymers, most conclude that the length of the side-chain has no effect on frontier orbital levels. However, in examining the data from these studies, we find that there is a slight tendency toward polymers with longer side-chains having deeper HOMOs (usually ≤ 0.05 eV),[32,33] a small but consistent trend that matches our observations from this study.

Space-charge limited current (SCLC) mobility measurements were performed on hole-only devices for the T-X-T/dtdDPP family of polymers. Films were cast from chloroform solutions, in which all the polymers readily dissolved, and devices were tested with and without thermal annealing. As in our first study, all the polymers exhibited improved performance after annealing, though only slightly (**Table 1, Tables S23-S24**). As before, the fully conjugated P3HTT-dtdDPP-10% had the best performance, increasing from 4.24 x 10^{-4} cm^2 V^{-1} s^{-1} to 6.11 x 10^{-4} cm^2 V^{-1} s^{-1} after annealing. Similar to our previous results[10] and a study by the Mei group,[3] charge mobilities were seen to steadily decrease with increasing CBS (and dtdDPP) content, attributed to the corresponding increase in insulating alkyl chains (**Figure S64-S65**). Again, this T-X-T/dtdDPP family of polymers showed an increase in charge mobility with increasing CBS length, in contrast to the observations of Zhao et al.[29] The observed trend is unexpected as a polymer with a more extended CBS monomer has more non-conjugated hydrocarbon than a polymer with shorter CBS units. We reason that longer spacers could imbue polymers with enhanced flexibility and therefore

facilitate rearrangement of the electroactive segments into a configuration favorable for charge transport. It is difficult to say if the apparent increase in crystalline order observed in the 40% T-4-T/40% dtdDPP and 40% T-8-T/40% dtdDPP GIXRD patterns after annealing aided charge transport in these polymers, as both polymers gave unreliable hole mobility data after annealing (**Table 1**). However, the as-cast films produced consistent hole mobility data that were the same order of magnitude as the annealed films, though slightly lower. In this polymer family, the fully conjugated P3HTT-dtdDPP-10% outperformed the CBS polymers by an order of magnitude or more, contrary to our previous study which found at least one CBS polymer (10% T-10-T) to perform comparably to the fully conjugated polymer.[10] Here, the 10% T-10-T/10% dtdDPP polymer again had the best performance of the CBS polymers, both before and after annealing.

While the SCLC hole mobilities for this dtdDPP family of polymers were diminished compared to the ehDPP family, the mechanical properties were enhanced. Because the entire family was readily soluble in chloroform and formed uniform films, the intrinsic mechanical properties of the freestanding films could be measured using the so-called film-on-water method developed by Kim et al[34] (**Table 2**). This method is a of a standard pull test (wherein a sample is suspended in air) where the film can move freely on the water surface (**Figure 2b**). Stress-strain curves were acquired for polymer thin films and from them were extracted the ultimate tensile strength (UTS); toughness; the tensile (Young's) modulus, *E*; and extensibility, or crack-onset strain (COS) (**Figure 2a**).[10] Representative optical images of films unstrained and strained until failure are shown in **Figure S73**. Films exhibiting brittle fracture (e.g., P3HTT-dtdDPP-10%) are characterized by long, narrow cracks, while those exhibiting greater ductility show only small microvoids, consistent with plastic flow and increased toughness.[35]

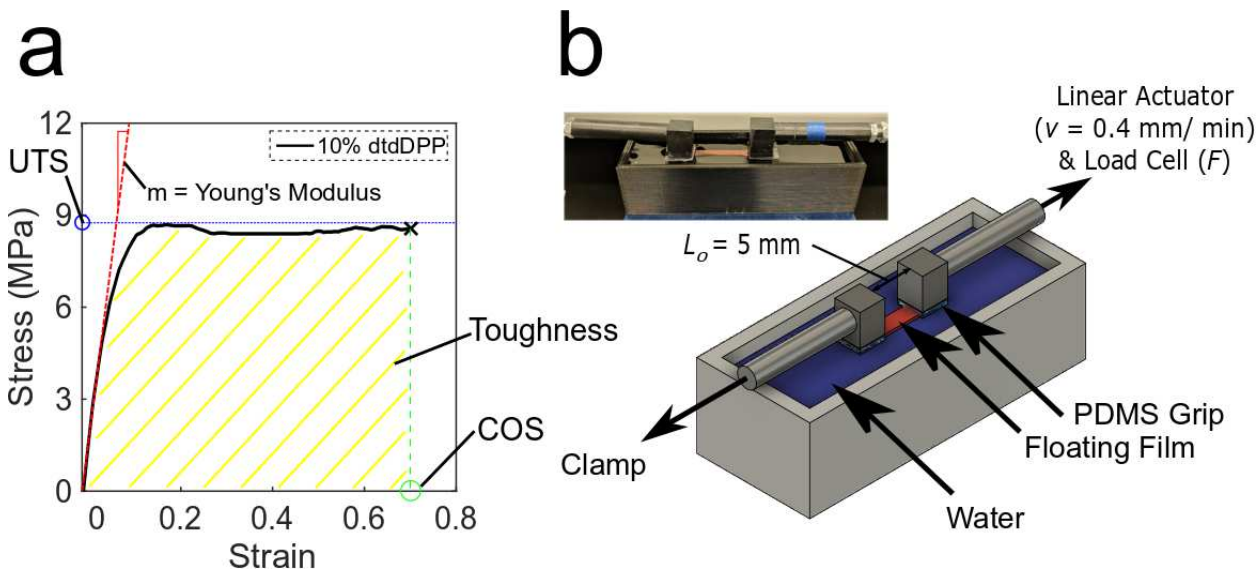

Figure 2. Overview of methodology used to measure the mechanical response. (a) From a stress–strain curve (black curve in the above graph is P3HTT-dtdDPP-10%), modulus (shown by the red dashed line) is the ratio of stress to strain in the linear regime of the curve, ultimate tensile strength (UTS) is the highest stress that the material exerts, toughness is the area under the entire stress–strain curve, and crack–onset–strain (COS) is the strain at which the material fractures. Stress–strain graphs are obtained by the film–on–water methodology, schematic representation shown in (b), which includes a floating film, linear actuator, clamp attached to a load cell, and a trough filled with water. The inset photograph is a demonstration of the real–life apparatus.

Table 2: Mechanical properties for decyltetradecyl DPP family

Polymer	Modulus (MPa)[a]	Toughness (MPa)[b]	UTS (MPa)[c]	Fracture Strength (MPa)[d]	Fracture Strain (%)[e]
P3HTT-dtdDPP-10%	104.17 ± 4.91	5.34 ± 1.02	8.68 ± 0.02	8.20 ± 0.55	68 ± 11
10% T-4-T/10% dtdDPP	-[f]	-[f]	-[f]	-[f]	-[f]
10% T-8-T/10% dtdDPP	19.68 ± 2.00	4.98 ± 0.27	3.61 ± 0.27	3.57 ± 0.32	185 ± 33
10% T-10-T/10% dtdDPP	15.34 ± 2.51	4.13 ± 1.06	2.15 ± 0.50	1.90 ± 0.80	217 ± 6
20% T-8-T/20% dtdDPP	15.07 ± 4.46	3.41 ± 1.30	2.63 ± 0.55	2.51 ± 0.55	185 ± 26
20% T-10-T/20% dtdDPP	5.45 ± 1.35	4.33 ± 0.34	1.77 ± 0.24	1.74 ± 0.32	357 ± 55
30% T-8-T/30% dtdDPP	14.84 ± 1.01	9.12 ± 2.00	4.49 ± 0.55	4.38 ± 0.67	325 ± 44
40% T-4-T/40% dtdDPP	38 ± 1	0.79 ± 0.06	1.77 ± 0.00	1.58 ± 0.05	53 ± 4
40% T-8-T/40% dtdDPP	27.39 ± 3.52	20.59 ± 1.33	8.45 ± 0.11	8.45 ± 0.04	398 ± 32

a) Derived from linear regime of stress–strain curves; b) Obtained by integrating the area under the stress–strain curve; c) Obtained from the maximum stress value in the stress–strain curve; d) Obtained from stress at failure; e) Obtained from strain at failure; f) Due to poor film integrity, no stress-strain curves could be obtained.

The fully conjugated P3HTT-dtdDPP-10% had an elastic modulus (0.104 GPa) less than half that of the fully conjugated ehDPP analog from the previous study, P3HTT-DPP-10% (0.32 GPa, measured via film-on-water),[10] a sign that the longer side-chains imbued the polymer with more ductility, a phenomenon that has previously been noted in the literature.[11,32,36] As another indication of ductility, the strain necessary to fracture the film (COS) was greatly enhanced to 68% in the polymer with longer side-chains on the DPP relative to only 10% for P3HTT-DPP-10% (measured via film-on-elastomer).

On the whole, this family of polymers had lower elastic moduli than the polymers analyzed in the previous study (**Figure 3d**) by at least an order of magnitude, with the 20% T-10-T/20%

dtdDPP polymer yielding a modulus as low as 5.45 MPa. This is nearing the modulus range expected from conventional elastomers like polyisoprene[16] or PDMS.[15] However, this polymer had a low charge mobility when measured by SCLC, typifying the tradeoff between mechanical and electronic properties so often witnessed in semiconducting polymers.[37] Surprisingly, the dtdDPP family of polymers was also slightly tougher than the original family, as shown in **Figures 3a** and **3c**, although this conclusion is difficult to definitively state due to the high standard deviations. Another factor that has been linked to improving the toughness of a material is an increase in the intermolecular forces between individual polymer chains.[37] In this case, we attribute the increased toughness of the longer side-chain containing polymers to the increase in extensibility these polymers exhibit (**Figure 3e**), with fracture strains as high as 398%. Finally, as shown in **Figure 3b**, the polymers with ehDPP consistently had a higher UTS than the counterpart polymers with the longer dtdDPP side-chain.

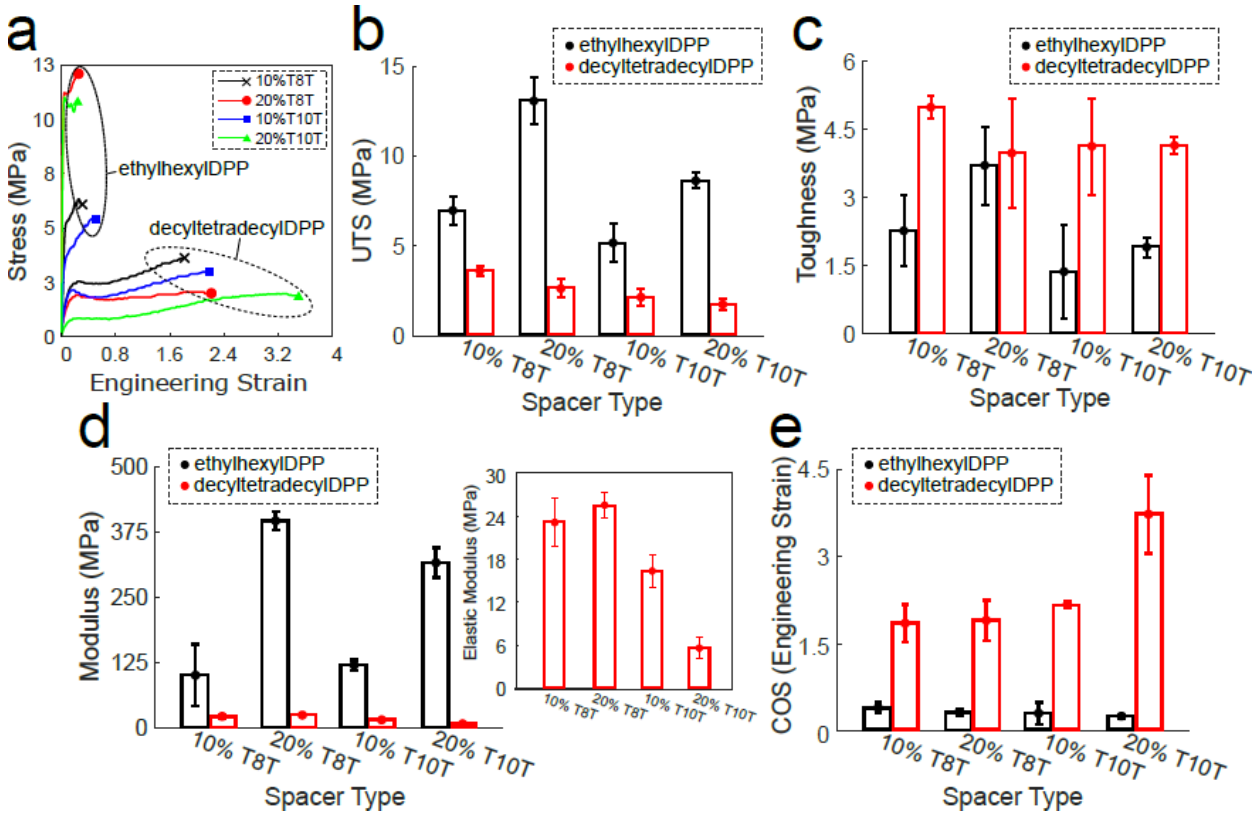

Figure 3. Comparative stress–strain graphs and mechanical properties for varying side chain lengths of 10% T-8-T, 20% T-8-T, 10% T-10-T, and 20% T-10-T. (a) Representative stress–strain graphs were obtained through film–on–water methodology with ethylhexyl DPP (ehDPP) and decyltetradecyl DPP (dtdDPP) curves grouped together. The resulting material properties, (b) ultimate tensile strength (UTS), (c) toughness, (d) modulus, and (e) crack-onset strain (COS), for different side-chain lengths on T-8-Ts and T-10-Ts are compared, with ethylhexyl DPP represented in black, and decyltetradecyl DPP represented in red. Mean values were obtained from conducting at least 3 film-on-water tests for each material and error bars were based on a 95% confidence bound. ehDPP data taken from Ref. 10.

Within the family of dtdDPP CBS polymers, several trends emerged. All of the CBS polymers had a lower elastic modulus than the fully conjugated P3HTT-dtdDPP-10% by an order of

magnitude (**Table S27, Figure S74**). The modulus appeared to decrease with longer conjugation-break spacers, a trend mirrored by the previous family with ethylhexyl side-chains. Within polymers of the same CBS length, moduli seemed to be consistent across spacer content until 40% CBS incorporation, at which point they increased slightly, perhaps due to an increase in the stiff DPP monomer content (**Table 2**). The 30% and 40% T-8-T/dtdDPP polymers had much higher toughness than the other polymers, including even the fully conjugated polymer, again perhaps attributable to the increase in DPP monomer content. The UTS and fracture strength were observed to generally decrease with longer spacers (**Tables S29-S30, Figures S76-S77**), indicating that though these materials were more extensible than polymers with shorter spacers, they were also slightly weaker. Within the T-8-T subfamily, UTS and fracture strength increased with 30% and 40% incorporation of the CBS and DPP monomer, until the 40% T-8-T/40% dtdDPP polymer had comparable UTS and fracture strength to the fully conjugated reference polymer. Other than 40% T-4-T/40% dtdDPP, the fracture strain increased with longer conjugation-break spacers and higher percent incorporation of CBS (**Table S31, Figure S78**), resulting in films able to withstand strains much higher than the reference P3HTT-dtdDPP-10% polymer and higher even than the CBS polymers tested within the first study.

Effects of increasing CBS content independent of DPP content

A family of five polymers with 10-50% CBS, 10% ehDPP, and 80-40% 3-hexylthiophene (3HT) incorporation (**Scheme 2b**) were synthesized via Stille polymerization, along with the reference polymer, P3HTT-DPP-10% (**Scheme 1**).[21] T-8-T was chosen as the CBS monomer to provide a full comparison to the dtdDPP series synthesized in the above study. DPP content was kept at 10% to minimize its negative effects on solubility and because the 10% DPP polymers from previous

studies had the highest charge mobility.[10] The side-chains on the DPP monomer were kept short (ethylhexyl instead of decyltetradecyl) because of the detrimental effects that long side-chains were shown to have on charge mobility (vide supra). Polymers were named for the CBS monomer length and content as well as the corresponding DPP monomer and its content. For example, a polymer with an 8-carbon CBS incorporated into the backbone at 30 mole, 10 mole percent of DPP, and 60 mole percent of 3HT would be named 30% T-8-T/10% ehDPP. ^{1}H NMR was used to confirm that the monomer feed ratios matched the polymer composition (**Figure S11-S12**). The average molecular weight for this family was low at 12.7 kDa, attributed to poor solubility (**Table 3, Table S3, Figure S3**). The low molecular weight and broad dispersity of the 20% T-8-T/10% ehDPP polymer is due to a bimodal weight distribution – the hexane Soxhlet performed to remove oligomers did not succeed in extracting the low molecular weight fraction from this polymer. Yields were generally greater than 60% (**Table S4, Figure S4**) with the exception of 50% T-8-T/10% ehDPP in which a great deal of solid remained in the Soxhlet thimble after extraction with chloroform. These solubility obstacles were not anticipated, because it was presumed that solubility would be enhanced by both keeping DPP content low and increasing CBS content. However, it is clear that the CBS units do not necessarily imbue a strong solubilizing power.

Table 3. SEC, thermal, optical, and electronic data for polymers with 10% ehDPP fixed content

Polymer	**M_n[a] (kDa)**	**Đ[a]**	**T_m / T_c[b] (°C)**	**E_g[c] (eV)**	**HOMO[d] (eV)**	**μ_h[e] ($cm^2 V^{-1} s^{-1}$)**
P3HTT-DPP-10%	10.5	4.31	211 / 207	1.49	5.39	9.29 E-4
10% T-8-T/10% ehDPP	19.7	6.23	- / -[f]	1.56	5.52	2.12 E-5
20% T-8-T/10% ehDPP	8.5	8.18	- / -[f]	1.59	5.48	7.05 E-6
30% T-8-T/10% ehDPP	12.8	3.75	- / -[f]	1.65	5.50	2.06 E-6
40% T-8-T/10% ehDPP	12.4	5.24	- / -[f]	1.68	5.63	-[g]
50% T-8-T/10% ehDPP	10.2	4.97	78 / 42	1.70	5.48	3.19 E-7

a) Obtained through size-exclusion chromatography (SEC); b) Obtained through differential scanning calorimetry (DSC); c) Calculated from the absorption onset in annealed thin films; d) Calculated from cyclic voltammetry (CV) oxidation onset; e) Calculated from charge carrier mobility measurements in the space charge limited current (SCLC) regime in hole-only devices in which the polymer thin film was spin-cast from chloroform and annealed for 30 min at 150 °C prior to cathode deposition; f) No thermal transitions observed; g) Not enough sample for hole mobility measurements.

The UV-vis spectra of the annealed polymers are shown in **Figure 1b**. In all cases, CBS-containing polymers had a wider optical bandgap and blue-shifted absorption onset relative to the P3HTT-DPP-10% reference polymer (**Table 3**). The absorption onset blue-shifted linearly as the content of dtdDPP and CBS the polymer increased, to a maximum onset of 1.70 eV with 50% T-8-T/10% ehDPP (**Figure S25**). Because the continuous conjugation of a conjugated polymer in effect draws the LUMO and HOMO nearer to each other, the bandgap of the material is lowered, explaining the tendency of these materials to blue-shift with increasing CBS incorporation. Interestingly, the bandgap did not increase as rapidly with CBS content in this set of polymers as with simultaneously increased DPP and CBS content (vide supra & ref. 10). For contrast, an earlier study on semi-random polymers found that the absorption onset red-shifted with increasing DPP

acceptor content in the absence of CBS units.[31] As such we had expected that by keeping the DPP content constant at 10 mole percent, the bandgap would increase more rapidly with increasing CBS content than in the study where DPP content rose simultaneously.

As CBS content increased, absorption from 400-550 nm (ascribed to P3HT rich segments) decreased, as expected, due to a concurrent decrease in loading of the 3-hexylthiophene content (**Figure 1b**). This was accompanied by an absorption peak that grew in at about 300-400 nm. This region is attributed to isolated bithiophene segments, which are likely to form in this semi-random system in which thiophene-terminated CBS monomers can bond with each other (**Scheme 2b**). Long wavelength absorption due to DPP (600-800 nm) was observed to decrease as CBS content increased. Despite the constant molar content of DPP, as the fraction of CBS increases (at the expense of 3HT), the mass fraction of DPP in the polymer chain decreases, diluting the chromophore and its optical density.

Though it is known that conjugated polymers typically have high crystallization and melting temperatures, it has been shown that incorporating CBS units into the polymers can dramatically decrease the temperature of these thermal transitions, even leading to melt processability.[3,4,29] However, the polymers in this sub-family seemed to be primarily amorphous when analyzed by DSC, with thermal transitions only being observed in the 50% T-8-T/10% ehDPP polymer. It could be that the addition of a fourth monomer into the polymerization system led to increased structural disorder, as has been seen in semi-random and random systems in the past.[21,38,39]

Crystallinity in annealed and as-cast polymer films was examined by grazing incidence x-ray diffraction (GIXRD). The diffraction peak intensity decreased dramatically across the 10%, 20%, and 30% T-8-T/10% ehDPP polymers in as-cast films (**Figure S53, Table S21**), corresponding to the decrease in 3HT content in those polymers. Surprisingly, after thermal annealing, only the 10%

T-8-T/10% ehDPP polymer exhibited a 100 diffraction peak, much reduced in intensity compared to its as-cast film (**Figure S54, Table S22**), though the fully conjugated P3HTT-DPP-10% polymer 100 peak increased in intensity after annealing. All of the polymers in this family had a smaller lamellar packing distance than P3HT (16.7 Å)[40], as previously observed in semi-random polymers,[22] but also a smaller lamellar packing distance than those polymers in which DPP content increased concurrently with CBS content.[10] It is likely that the branched side-chains on the DPP monomer maintained interchain distance in the original family of polymers, while the polymers in this study with a constant low content of DPP could pack closer because of a relative decrease in branched side-chains.

The HOMO energy of each polymer was estimated from the onset of oxidation from cyclic voltammetry (CV). No trends were observed in the HOMOs of these polymers, as demonstrated by the data presented in **Table 3** and **Figure S33**. When averaged across the five CBS polymers in this study, the HOMO was 5.52 ± 0.06 eV, which is nearly within the measurement error range of ± 0.05 eV. This average CBS polymer HOMO was slightly deeper than the reference polymer, P3HTT-DPP-10%.

Charge carrier mobility was measured by the space-charge limited current (SCLC) technique in hole-only devices to gauge the polymers' potential utility in organic electronic devices. As observed by Zhao et al,[3] hole mobility decreased logarithmically with increasing CBS content (**Table 3, Figure S72**). This was a more dramatic trend than the decrease in charge mobility observed in either our previous study or the side-chain study above, in which CBS and DPP content increased concurrently. This led us to infer that despite a negative influence on solubility and processability, the DPP monomer contributes significantly to the electronic properties of the

polymer. Similar to what we observed in previous studies, the charge mobilities generally increased upon thermal annealing, with the exception of the 50% T-8-T/10% ehDPP polymer.

In an effort to understand the mechanical properties that would affect the behavior of these polymers in a flexible electronic device, film-on-water mechanical testing was performed, with the data summarized in **Table 4**. Due to poor film integrity, measurements could not be completed on the 50% T-8-T/10% ehDPP polymer. In looking at the stress–strain curves in **Figure 4a**, the first thing to notice is how noisy the curves are and how the polymers never seem to plastically deform, unlike the curves for the T-8-T polymers with matched dtdDPP content in **Figure 4b**, which are smooth. This variation is perhaps because increasing the percentage of the spacer while holding the fraction of the rigid DPP segment constant allows for the material to behave more like a rubber as the relative ratio of DPP to CBS decreases. From the film-on-water tests, we learned that increasing the CBS content while keeping the DPP content at 10% led to a logarithmic decrease in elastic modulus, *E* (**Figure S79**). This is contrary to the effect observed in our first study, in which increasing CBS and DPP content simultaneously led to a slight increase in elastic modulus. The modulus for the 40% T-8-T/10% ehDPP polymer is as low as 4.08 MPa, again close to the range of conventional elastomers like PDMS.[15] Unfortunately there was not enough of the material to complete charge mobility tests, though the trends lead us to speculate that polymer would have a value in the high 10^{-7} cm^2 V^{-1} s^{-1} in annealed films, another example of the pervasive trade-off between mechanical and electronic properties in semiconducting polymers.[37]

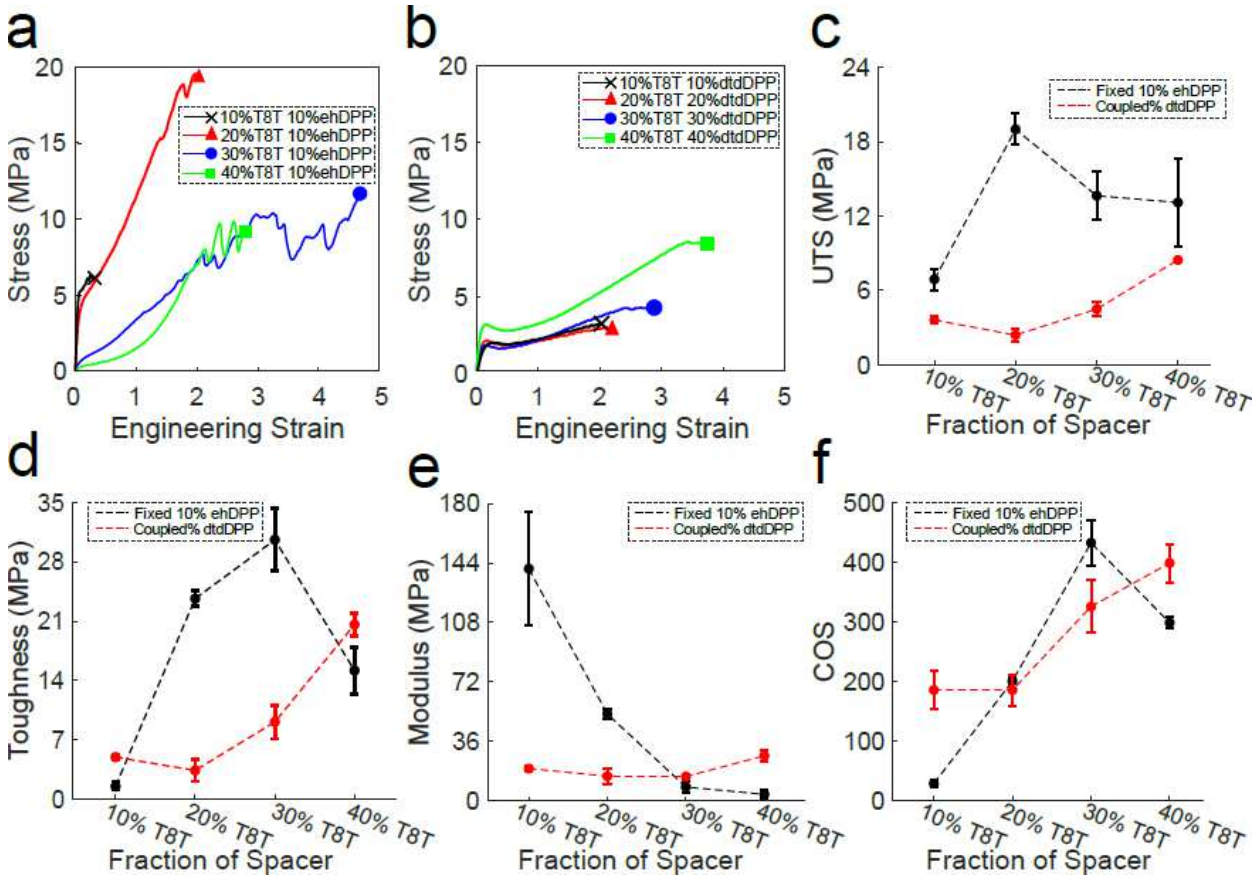

Figure 4. Comparative stress–strain curves and mechanical properties of polymers with constant and variable percentages of DPP obtained through the film–on–water technique. (a) Stress–strain curves of polymers with the percentage of ehDPP held constant and (b) polymers with the percentage of dtdDPP and CBS coupled together. Dotted lines are used to guide the eyes, while the black lines are used to represent the polymers with constant 10% ehDPP, and the red lines are used to depict the polymers with a dtdDPP fraction that matches the fraction of the spacer– referred to as "coupled" in the legends. The resulting mechanical properties (c) UTS, (d) toughness, (e) modulus, and (f) COS of the polymers with variable and constant DPP percentage are compared. Mean values were obtained from conducting at least 3 film–on–water tests for each material and error bars were based on a 95% confidence bound.

Table 4. Mechanical properties for polymer family with 10% ehDPP fixed content

Polymer	Modulus (MPa)[a]	Toughness (MPa)[b]	UTS (MPa)[c]	Fracture Strength (MPa)[d]	Fracture Strain (%)[e]
10% T-8-T/10% ehDPP	140.50 ± 34.20	1.54 ± 0.52	6.89 ± 0.85	6.6 ± 0.5	28 ± 6
20% T-8-T/10% ehDPP	52.70 ± 2.82	23.65 ± 0.89	18.99 ± 1.26	18.73 ± 1.25	200 ± 5
30% T-8-T/10% ehDPP	8.54 ± 3.21	30.57 ± 3.66	13.63 ± 1.86	12.74 ± 0.62	432 ± 38
40% T-8-T/10% ehDPP	4.08 ± 2.37	15.18 ± 2.75	13.09 ± 3.58	9.97 ± 4.78	298 ± 10
50% T-8-T/10% ehDPP	-[f]	-[f]	-[f]	-[f]	-[f]

a) Derived from linear regime of stress–strain curves; b) Obtained by integrating the area under the stress–strain curve; c) Obtained from the maximum stress value in the stress–strain curve; d) Obtained from stress at failure; e) Obtained from strain at failure; f) Due to poor film integrity, no stress-strain curves could be obtained.

While it becomes difficult to draw comparisons between the ehDPP and dtdDPP polymers, analyzing these results in context of the results presented in **Figure 3** allows more insight. For example, as shown in **Figure 3b,** the polymers with ehDPP had a significantly higher UTS than those polymers with dtdDPP when the fraction of DPP was coupled with the fraction of the spacer. In looking at **Figure 4c**, we notice that the UTS of the polymers with a constant 10% ehDPP is still greater than those with a fraction of dtdDPP matching that of the CBS. Additionally, as determined in our previous study, increasing the fraction of DPP and the spacer will increase the UTS;[10] however, as shown in **Figure 4c**, there is a slight decrease after 20% T-8-T 10% ehDPP, which could suggest that increasing only the fraction of the spacer while holding the DPP constant will relatively decrease the UTS of the material.

Unlike UTS and toughness, modulus appears to have a different trend between polymers with fixed and variable DPP content. As determined in the previous study, there is an increase in the modulus as the percentage of the spacer and DPP increases.[10] This relationship is also observed in

Figure 4e: as the percentage of the DPP and spacer increase concurrently, the modulus increases. Conversely, when only the percentage of the CBS is increased and the DPP content is fixed, there is a dramatic decrease in the modulus, as shown by the black dashed line in **Figure 4e**, which suggests that as only the percentage of the CBS increases, the modulus will decrease.

In general, this family of polymers showed increased toughness relative to the original ehDPP family in our first study. Again, we attribute the increased toughness of the polymers to the increase in extensibility these polymers exhibit, with fracture strains as high as 432%. The toughness had a slight tendency to increase with increasing CBS monomer incorporation (**Figure 4d, Figure S80**), mirroring the rise in fracture strain observed for the 10%, 20%, and 30% T-8-T/10% DPP polymers (**Figure 4f, Figure S83**). Fracture strain in these samples far exceeded those values obtained in our first study, with films able to extend several times beyond their original length before fracturing.

When compared to the film-on-elastomer modulus (0.32 GPa) and crack-onset strain (10%) measured for the fully conjugated reference polymer P3HTT-DPP-10% in the original study, all of the polymers examined here have superior mechanical properties. Materials such as these exhibiting both high fracture (or crack-onset) strains and low elastic moduli are expected to deform more easily and produce less interfacial stress in a multi-layered device, reducing the likelihood of device failure by interfacial delamination.[37] For this reason, they are generally regarded as better for use in flexible electronics applications.

Conclusions:

In this work, two families of semi-random CBS polymers were synthesized to overcome the limitations of the original polymers synthesized for our first study and to expand the understanding

of structure-function relationships in the mechanical and electronic properties of semi-random CBS polymers. In one study, a set of semi-random polymers with varying lengths and compositions of conjugation-break spacers and decyltetradecyl-substituted DPP monomers were synthesized and analyzed for optoelectronic and mechanical properties. This family was a derivative of the previous polymer family and was designed with the aim of improving solubility, and thus film-forming ability. Succeeding in this aim, these polymers had much higher solubility than the original family and could attain higher molecular weights and form films with high integrity. These polymers displayed extraordinary mechanical properties, with elastic moduli as low as 5.45 MPa and fracture strains as high as 398%, though these remarkable mechanical properties came at the expense of electronic properties, with lower hole mobilities than the previous family. This study indicates that a favorable balance between mechanical and electronic properties could be struck with side-chains of a middling length, between ethylhexyl and decyltetradecyl.

Additionally, a series of semi-random polymers with a constant 10% ehDPP and varying amounts of conjugation-break spacer was synthesized and analyzed for optoelectronic and mechanical properties. The data presented herein served to disentangle the effects of increasing CBS and DPP content simultaneously. Polymer solubility, molecular weight, and processability were not shown to improve dramatically compared to those polymers in the previous study that varied the DPP content, indicating that the DPP monomer content was not the only factor hampering solubility. SCLC hole mobilities in this family of polymers dropped more rapidly as CBS content increased than in the family where CBS and DPP content increased concurrently, signifying that the DPP monomer contributed significantly to charge mobility. Finally, the mechanical properties of this series of polymers were quite notable, with elastic moduli as low as 4.08 MPa, an increase in

toughness, and fracture strains as high as 432%. These observations indicated that the DPP monomer, while beneficial to the electronic properties of the polymers, indeed was responsible for undesirable mechanical properties. The extraordinary mechanical properties exhibited by the polymers presented herein can serve as a guide in the judicious selection of monomers and backbone architectures in the future synthesis of semiconducting polymers for flexible electronic applications.

Supporting Information Available:

General synthetic methods, materials, and characterization methods; synthetic data; polymer and small molecule NMR spectra; UV-Vis absorption spectra and optical data; cyclic voltammograms and oxidation data; differential scanning calorimetry plots and melting/crystallization data; GIXRD patterns and data; SCLC hole mobility curves and data; film-on-water mechanical data and images.

Corresponding Author

*Barry C. Thompson (barrycth@usc.edu).

*Darren J. Lipomi (dlipomi@eng.ucsd.edu).

Author Contributions

The manuscript was written through contributions of all authors. All authors have given approval to the final version of the manuscript.

ACKNOWLEDGMENT:

BCT acknowledges support by the National Science Foundation (CBET Energy for Sustainability) CBET-1803063. D.J.L. acknowledges support from the Air Force Office of Scientific Research Grant FA9550-16-1-0220.

References

1. Schroeder, B. C.; Chiu, Y.; Gu, X.; Zhou, Y.; Xu, J.; Lopez, J.; Lu, C.; Toney, M. F.; Bao, Z. Non-Conjugated Flexible Linkers in Semiconducting Polymers: A Pathway to Improved Processability without Compromising Device Performance. *Adv. Electron. Mater.* **2016***, 2*, 1600104.

2. Wang, G. N.; Molina-Lopez, F.; Zhang, H.; Xu, J.; Wu, H.; Lopez, J.; Shaw, L.; Mun, J.; Zhang, Q.; Wang, S.; Ehrlich, A.; Bao, Z. Nonhalogenated Solvent Processable and Printable High-Performance Polymer Semiconductor Enabled by Isomeric Nonconjugated Flexible Linkers. *Macromolecules* **2018***, 51*, 4976-4985.

3. Zhao, Y.; Zhao, X.; Zang, Y.; Di, C.; Diao, Y.; Mei, J. Conjugation-Break Spacers in Semiconducting Polymers: Impact on Polymer Processability and Charge Transport Properties. *Macromolecules* **2015***, 48*, 2048-2053.

4. Zhao, Y.; Zhao, X.; Roders, M.; Gumyusenge, A.; Ayzner, A. L.; Mei, J. Melt-Processing of Complementary Semiconducting Polymer Blends for High Performance Organic Transistors. *Adv. Mater.* **2016***, 29*, 1605056.

5. Li, H.; Wang, J.; Mei, C.; Li, W. A New Class of Organic Photovoltaic Materials: Poly(Rod-Coil) Polymers having Alternative Conjugated and Non-Conjugated Segments. *Chem. Commun.* **2014***, 50*, 7720-7722.

6. Shao, W.; Liang, L.; Xiang, X.; Li, H.; Zhao, F.; Li, W. Changing to Poly(Rod-coil) Polymers: A Promising Way for an Optoelectronic Compound to Improve its Film Formation. *Chin. J. Chem.* **2015***, 33*, 847-851.

7. Xiang, X.; Shao, W.; Liang, L.; Chen, X.; Zhao, F.; Lu, Z.; Wang, W.; Li, J.; Li, W. Photovoltaic Poly(Rod-Coil) Polymers Based on Benzodithiophene-Centred A–D–A Type Conjugated Segments and Dicarboxylate-Linked Alkyl Non-Conjugated Segments. *RSC Adv.* **2016***, 6*, 23300-23309.

8. Savagatrup, S.; Zhao, X.; Chan, E.; Mei, J.; Lipomi, D. J. Effect of Broken Conjugation on the Stretchability of Semiconducting Polymers. *Macromol. Rapid Commun.* **2016***, 37*, 1623-1628.

9. Oh, J. Y.; Rondeau-Gagné, S.; Chiu, Y.; Chortos, A.; Lissel, F.; Wang, G. N.; Schroeder, B. C.; Kurosawa, T.; Lopez, J.; Katsumata, T.; Xu, J.; Zhu, C.; Gu, X.; Bae, W.; Kim, Y.; Jin, L.; Chung, J. W.; Tok, J. B. -.; Bao, Z. Intrinsically Stretchable and Healable Semiconducting Polymer for Organic Transistors. *Nature* **2016***, 539*, 411-415.

10. Melenbrink, E. L.; Hilby, K. M.; Alkhadra, M. A.; Samal, S.; Lipomi, D. J.; Thompson, B. C. Influence of Systematic Incorporation of Conjugation-Break Spacers into Semi-Random Polymers on Mechanical and Electronic Properties. *ACS Appl. Mater. Interfaces* **2018***, 10*, 32426-32434.

11. Savagatrup, S.; Makaram, A. S.; Burke, D. J.; Lipomi, D. J. Mechanical Properties of Conjugated Polymers and Polymer-Fullerene Composites as a Function of Molecular Structure. *Adv. Funct. Mater.* **2014***, 24*, 1169-1181.

12. Roth, B.; Savagatrup, S.; V. de los Santos, Nathaniel; Hagemann, O.; Carlé, J. E.; Helgesen, M.; Livi, F.; Bundgaard, E.; Søndergaard, R. R.; Krebs, F. C.; Lipomi, D. J. Mechanical Properties of a Library of Low-Band-Gap Polymers. *Chem. Mater.* **2016***, 28*, 2363-2373.

13. Printz, A. D.; Savagatrup, S.; Burke, D. J.; Purdy, T. N.; Lipomi, D. J. Increased Elasticity of a Low-Bandgap Conjugated Copolymer by Random Segmentation for Mechanically Robust Solar Cells. *RSC Adv.* **2014**, *4*, 13635-13643.

14. Zhou, J.; Qiang Li, E.; Li, R.; Xu, X.; Aguilar Ventura, I.; Moussawi, A.; H. Anjum, D.; Nejib Hedhili, M.; Smilgies, D.; Lubineau, G.; T. Thoroddsen, S. Semi-Metallic, Strong and Stretchable Wet-Spun Conjugated Polymer Microfibers. *J. Mater. Chem. C* **2015**, *3*, 2528-2538.

15. Khanafer, K.; Duprey, A.; Schlicht, M.; Berguer, R. Effects of Strain Rate, Mixing Ratio, and Stress–strain Definition on the Mechanical Behavior of the Polydimethylsiloxane (PDMS) Material as Related to its Biological Applications. *Biomed. Microdevices* **2009**, *11*, 503-508.

16. Baboo, M.; Dixit, M.; Sharma, K.; Saxena, N. Mechanical and Thermal Characterization of Cis-Polyisoprene and Trans-Polyisoprene Blends. *Polym. Bull.* **2011**, *66*, 661-672.

17. Howard, J. B.; Thompson, B. C. Design of Random and Semi-Random Conjugated Polymers for Organic Solar Cells. *Macromol. Chem. Phys.* **2017**, *218*, 1700255.

18. Howard, J. B.; Ekiz, S.; Noh, S.; Thompson, B. C. Surface Energy Modification of Semi-Random P3HTT-DPP. *ACS Macro Lett.* **2016**, *5*, 977-981.

19. O'Connor, B.; Chan, E. P.; Chan, C.; Conrad, B. R.; Richter, L. J.; Kline, R. J.; Heeney, M.; McCulloch, I.; Soles, C. L.; DeLongchamp, D. M. Correlations between Mechanical and Electrical Properties of Polythiophenes. *ACS Nano* **2010**, *4*, 7538-7544.

20. Awartani, O.; Lemanski, B. I.; Ro, H. W.; Richter, L. J.; DeLongchamp, D. M.; O'Connor, B. T. Correlating Stiffness, Ductility, and Morphology of Polymer:Fullerene Films for Solar Cell Applications. *Adv. Energy Mater.* **2013**, *3*, 399-406.

21. Burkhart, B.; Khlyabich, P. P.; Cakir Canak, T.; LaJoie, T. W.; Thompson, B. C. “Semi-Random” Multichromophoric Rr-P3HT Analogues for Solar Photon Harvesting. *Macromolecules* **2011***, 44*, 1242-1246.

22. Khlyabich, P. P.; Burkhart, B.; Ng, C. F.; Thompson, B. C. Efficient Solar Cells from Semi-Random P3HT Analogues Incorporating Diketopyrrolopyrrole. *Macromolecules* **2011***, 44*, 5079-5084.

23. Sugiyama, F.; Kleinschmidt, A. T.; Kayser, L. V.; Rodriquez, D.; Finn, M.; Alkhadra, M. A.; Wan, J. M. -.; Ramírez, J.; Chiang, A. S. -.; Root, S. E.; Savagatrup, S.; Lipomi, D. J. Effects of Flexibility and Branching of Side Chains on the Mechanical Properties of Low-Bandgap Conjugated Polymers. *Polym. Chem.* **2018***, 9*, 4354-4363.

24. Lee, J.; Han, A.; Yu, H.; Shin, T. J.; Yang, C.; Oh, J. H. Boosting the Ambipolar Performance of Solution-Processable Polymer Semiconductors Via Hybrid Side-Chain Engineering. *J. Am. Chem. Soc.* **2013***, 135*, 9540-9547.

25. Mei, J.; Bao, Z. Side Chain Engineering in Solution-Processable Conjugated Polymers. *Chem. Mater.* **2014***, 26*, 604-615.

26. Kang, I.; Yun, H.; Chung, D. S.; Kwon, S.; Kim, Y. Record High Hole Mobility in Polymer Semiconductors Via Side-Chain Engineering. *J. Am. Chem. Soc.* **2013***, 135*, 14896-14899.

27. Ma, Z.; Geng, H.; Wang, D.; Shuai, Z. Influence of Alkyl Side-Chain Length on the Carrier Mobility in Organic Semiconductors: Herringbone Vs. Pi–pi Stacking. *J. Mater. Chem. C* **2016***, 4*, 4546-4555.

28. Gruber, M.; Jung, S.; Schott, S.; Venkateshvaran, D.; Kronemeijer, A. J.; Andreasen, J. W.; Mcneill, C. R.; Wong, W. W. H.; Shahid, M.; Heeney, M.; Lee, J.; Sirringhaus, H. Enabling High-Mobility, Ambipolar Charge-Transport in a DPP-Benzotriazole Copolymer by Side-Chain Engineering. *Chem. Sci.* **2015***, 6*, 6949-6960.

29. Zhao, X.; Zhao, Y.; Ge, Q.; Butrouna, K.; Diao, Y.; Graham, K. R.; Mei, J. Complementary Semiconducting Polymer Blends: The Influence of Conjugation-Break Spacer Length in Matrix Polymers. *Macromolecules* **2016***, 49*, 2601-2608.

30. Afifi-Effat, A. M.; Hay, J. N. Enthalpy and Entropy of Fusion and the Equilibrium Melting Point of Polyethylene Oxide. *J. Chem. Soc., Faraday Trans. 2* **1972***, 68*, 656-661.

31. Ekiz, S.; Gobalasingham, N. S.; Thompson, B. C. Exploring the Influence of Acceptor Content on Semi-random Conjugated Polymers. *J. Polym. Sci., Part A: Polym. Chem.* **2017***, 55*, 3884-3892.

32. Heintges, G. H. L.; Leenaers, P. J.; Janssen, R. A. J. The Effect of Side-Chain Substitution and Hot Processing on Diketopyrrolopyrrole-Based Polymers for Organic Solar Cells. *J. Mater. Chem. A* **2017***, 5*, 13748-13756.

33. Duan, C.; Willems, R. E. M.; van Franeker, J. J.; Bruijnaers, B. J.; Wienk, M. M.; Janssen, R. A. Effect of Side Chain Length on the Charge Transport, Morphology, and Photovoltaic Performance of Conjugated Polymers in Bulk Heterojunction Solar Cells. *J. Mater. Chem. A* **2016***, 4*, 1855-1866.

34. Kim, J.; Nizami, A.; Hwangbo, Y.; Jang, B.; Lee, H.; Woo, C.; Hyun, S.; Kim, T. Tensile Testing of Ultra-Thin Films on Water Surface. *Nat. Commun.* **2013***, 4*, 2520.

35. Alkhadra, M. A.; Root, S. E.; Hilby, K. M.; Rodriquez, D.; Sugiyama, F.; Lipomi, D. J. Quantifying the Fracture Behavior of Brittle and Ductile Thin Films of Semiconducting Polymers. *Chem. Mater.* **2017***, 29*, 10139–10149.

36. Rodriquez, D.; Kim, J.; Root, S. E.; Fei, Z.; Boufflet, P.; Heeney, M.; Kim, T.; Lipomi, D. J. Comparison of Methods for Determining the Mechanical Properties of Semiconducting Polymer Films for Stretchable Electronics. *ACS Appl. Mater. Interfaces* **2017***, 9*, 8855-8862.

37. Savagatrup, S.; Printz, A. D.; Rodriquez, D.; Lipomi, D. J. Mechanical Properties of Organic Semiconductors for Stretchable, Highly Flexible, and Mechanically Robust Electronics. *Chem. Rev.* **2017***, 117*, 6467-6499.

38. Burkhart, B.; Khlyabich, P. P.; Thompson, B. C. Semi-Random Two-Acceptor Polymers: Elucidating Electronic Trends through Multiple Acceptor Combinations. *Macromol. Chem. Phys.* **2013***, 214*, 681-690.

39. Kang, S.; Kumari, T.; Lee, S. M.; Jeong, M.; Yang, C. Densely Packed Random Quarterpolymers Containing Two Donor and Two Acceptor Units: Controlling Absorption Ability and Molecular Interaction to Enable Enhanced Polymer Photovoltaic Devices. *Adv. Energy Mater.* **2017***, 7*, 1700349.

40. Verploegen, E.; Mondal, R.; Bettinger, C. J.; Sok, S.; Toney, M. F.; Bao, Z. Effects of Thermal Annealing upon the Morphology of Polymer–Fullerene Blends. *Adv. Funct. Mater.* **2010***, 20*, 3519-3529.

TOC GRAPHIC

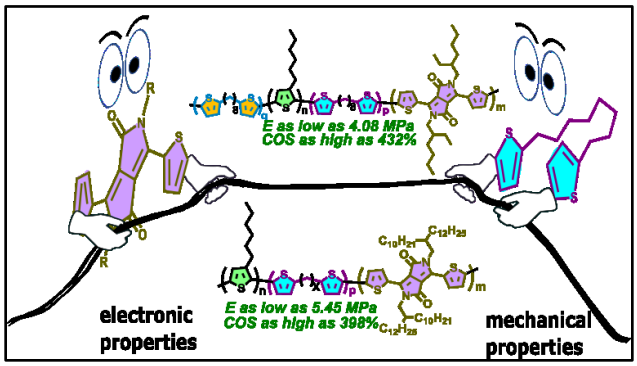
E as low as 4.08 MPa
COS as high as 432%
E as low as 5.45 MPa
COS as high as 398%
electronic properties
mechanical properties